Sizing the length of surface breaking cracks using vibrothermography

C. Cavallone[1-2], M. Colom[1], A. Mendioroz[1], A. Salazar[1], D. Palumbo[2], U. Galietti[2]

[1]Departamento de Física Aplicada I, Escuela de Ingeniería de Bilbao, Universidad del País Vasco UPV/EHU, Plaza Ingeniero Torres Quevedo 1, 48013 Bilbao, Spain.

[2]Politecnico di Bari, Department of Mechanics, Mathematics and Management, Viale Japigia 182, 70126 Bari, Italy.

[*]Corresponding author E-mail address: arantza.mendioroz@ehu.eus

Abstract

Ultrasound excited thermography is used to determine the length of vertical surface breaking cracks. Two methods are proposed based on the analysis of the maximum temperature reached along the line containing the crack and the time at which the maximum temperature occurs. It is shown that, for short bursts, the full width at half maximum of the maximum temperature curve provides the crack length, and that the time at which the maximum temperature occurs increases beyond the crack tip. The range of application of the methods is analysed and the validity is checked taking data on samples containing artificial calibrated cracks.

Keywords: crack length, vibrothermography, infrared thermography, non-destructive evaluation.

1. Introduction

Determining the length of fatigue cracks is a key aspect to understand and predict the mechanical behaviour of a structural component. This is the case, for example, of aerospace structures that must be developed in accordance to damage tolerance design principles [1]. This approach assumes an initial damage condition of the structure and an inspection schedule for controlling the damage evolution during the life of the structure. In this regard, non-destructive techniques such as eddy current, ultrasound, x-ray, dye penetrant and infrared thermography (IRT) [2-5] can be used to assess the size of the defect. In particular, IRT offers advantages, such as being contactless and full-field, that can significantly reduce the time of the maintenance checks [2].

Optically excited infrared thermography with laser spot excitation has demonstrated capabilities to quantify the width of infinite vertical cracks, both in lock-in and burst regimes [6-9]. In this technique, a lateral heat flow is induced across the crack by heating one side of the crack with a focused laser spot. The crack acts as a thermal resistance that hinders heat propagation and it is detected as a surface temperature discontinuity. By exciting the sample with multiple spots at different locations, it is possible to obtain a picture of the crack intersection with the sample surface [10-11], from which the crack length can be estimated. However, should the location of the crack be unknown, this method requires scanning the specimen surface with multiple excitations, which might be time consuming when inspecting large parts. Moreover, kissing cracks with very narrow average distances between lips might remain undetected because of the low thermal resistance they produce [8-9].

On the contrary, ultrasound excited infrared thermography (UET), also known as vibrothermography, provides full volume excitation and wide field inspection in a single experiment, being very adequate to reveal kissing cracks in a non-destructive way. In this technique, the sample is excited with ultrasounds. If there is a crack, the relative motion between the two crack faces produces heat, so the defect behaves as a heat source. This thermal energy propagates in the material and reaches the sample surface, producing a temperature elevation measurable with an infrared video camera, that reveals the presence of the crack. UET has successfully been applied to detect impact damage in composite structures [12-15] and to detect fatigue cracks in metallic laminates [16-18] as well as in massive metallic parts [19-21]. For a recent review see [22].

UET has already been applied to identify the heat flux distribution generated by surface breaking and buried vertical cracks, both in lock-in [21-24] and burst regimes [27-29]. Some of these works deal with kissing cracks (crack lips in contact), which typically generate heat all along the crack surface. In the case of homogeneous heat production along the crack lips, it has been shown that the geometry of the crack can be retrieved from UET experiments by inverting surface temperature data [23-25,27]. Moreover, in burst experiments, quantification of the absolute heat flux distribution and power generated at the crack has been carried out not only for homogeneous heat sources but also for cracks that produce inhomogeneous heat distributions [28]. In these works, the surface temperature distribution generated by the presence of the crack is inverted to retrieve the flux distribution responsible for the observed data, without previous knowledge of the geometry of the crack. Due to the severely ill-posed character of heat diffusion problems, the identification of the heat flux distribution in UET requires solving a minimization problem that is very unstable. This issue can be successfully solved [23-28], but it requires the implementation of sophisticated stabilizing techniques of the minimization procedure.

Very recently, a new methodology has been proposed to determine the length of the crack from burst UET data [30]. The authors present an analytical expression to calculate the surface temperature produced by an infinitely deep crack and they address the inversion by proposing a so-called “crack function” which is basically a residual built from surface temperature data in the area surrounding the crack at a given time in the image sequence. Again, this approach requires implementing a minimization algorithm.

In this work, we propose a simple methodology to identify the length of planar surface breaking cracks from burst vibrothermography data, without making use of sophisticated mathematical techniques. We identify the length of the region that actually produces heat and we assume that heat is produced all along the crack surface, i.e. the closure stresses are not strong enough to prevent heat production near the crack border. We propose two complementary methods to determine the length of the crack that do not involve complicated inversion algorithms. The methods are based on the analysis of the image sequence to identify the maximum temperature reached at each pixel of the profile containing the crack, and the time at which this maximum temperature occurs. The methodology aims at overcoming the difficulty of determining the crack length from the raw image sequence, due to heat diffusion. As a result of the diffusion process, the heat source generated at the crack in UET produces a blurred temperature elevation at the

surface, which significantly complicates the task of identifying the crack length. This issue is specific of UET as in other thermographic techniques aimed at detecting vertical cracks, such as laser spot thermography, the signature of the crack is a temperature discontinuity, which is not washed out by diffusion. In the following sections, we present a theoretical analysis to determine the range of burst durations for which the methods work and to estimate the precision on the extracted crack length depending on the thermal properties of the material, the duration of the burst and the crack length itself. Finally, we apply the methodology to determine the length of artificial calibrated cracks in AISI-304 samples excited with burst vibrothermography. The experiments were conducted with an IR camera equipped with a 320 x 240 pixels detector and a regular 50 mm focal length lens providing a spatial resolution of 140 μm, far from state of the art resolutions of up to 10 μm. The results demonstrate the applicability of the methods to UET experimental data obtained with inexpensive cameras.

2. Theoretical framework

We consider a rectangular surface breaking crack of length l and penetration h, contained in plane $x = 0$, perpendicular to the surface ($z = 0$) of a semi-infinite sample of thermal diffusivity and conductivity D and K, respectively. The geometry of the problem is sketched in Figure 1.

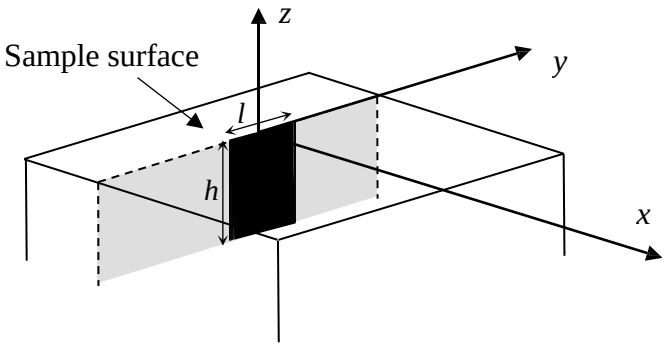

Figure 1. Geometry of the problem: a surface breaking rectangular crack of length l and penetration h is contained in plane $x = 0$, perpendicular to the sample surface, $z = 0$.

In the absence of heat losses, the evolution of the surface temperature distribution produced by a uniform flux I flowing from the crack, when excited by an ultrasound burst of duration τ, can be written as [31]:

$$T(x,y,0,t)=\frac{I}{2\pi K}\int_{-h}^{0}\int_{-l/2}^{-l/2}\frac{Erfc\left[\frac{\sqrt{x^2+(y-y')^2+z'^2}}{\sqrt{4Dt}}\right]}{\sqrt{x^2+(y-y')^2+z'^2}}dy'\,dz' \qquad 0\le t\le\tau \qquad (1a)$$

$$T(x,y,0,t)=\frac{I}{2\pi K}\Bigg[\int_{-h}^{0}\int_{-l/2}^{-l/2}\frac{Erfc\left[\frac{\sqrt{x^2+(y-y')^2+z'^2}}{\sqrt{4Dt}}\right]}{\sqrt{x^2+(y-y')^2+z'^2}}dy'\,dz'- \int_{-h}^{0}\int_{-l/2}^{-l/2}\frac{Erfc\left[\frac{\sqrt{x^2+(y-y')^2+z'^2}}{\sqrt{4D(t-\tau)}}\right]}{\sqrt{x^2+(y-y')^2+z'^2}}dy'\,dz'\Bigg] \qquad t>\tau \qquad (1b)$$

In the following, we consider that the penetration of the crack is infinite, $h=\infty$. Later in this section, the effect of the finite penetration of the crack will be analysed.

Equations 1 predict the evolution of the temperature distribution on the surface of the sample. In order to estimate the length of the crack, we make use of the information with the optimum signal-to-noise ratio (SNR): we focus on the surface temperature profile along the *OY* axis (see Figure 1), coinciding with the direction of the crack, and we extract two quantities: the maximum temperature reached at each position T_{max}, and the time at which that maximum temperature occurs t_{max}. As an example, in Figure 2 we compare the evolution of the surface temperature produced by a l = 3 mm long crack in AISI-304 steel (D = 4 mm^2/s, K = 16 Wm^{-1}K^{-1}) at two positions on top of the crack (the center (0,0,0), and position (0,1,0) (mm)), and another position beyond the crack tip, at (0, 2, 0) (mm). We present the calculation for two bursts of durations τ = 0.1 and 0.5 s. The temperatures T_n are normalized to the temperature obtained at the center of the crack at the end of the burst $T_n=\frac{T(0,y,0,t)}{T(0,0,0,\tau)}$.

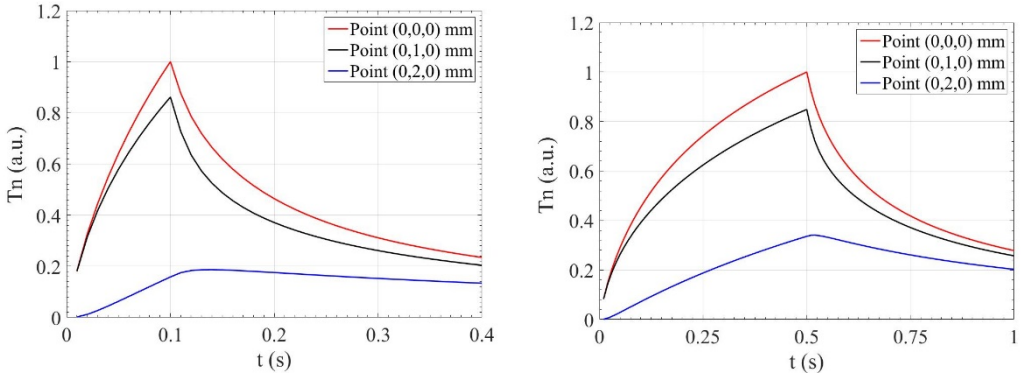

(a) (b)

Figure 2. Evolution of the temperature produced by a l = 3 mm long crack in AISI-304 at three positions, (0,0,0), (0,1,0), and (0,2,0) (mm), produced by bursts of duration (a) τ = 0.1 s and (b) τ = 0.5 s

The inspection of figure 2 shows that, at two positions within the crack, namely (0,0,0) and (0,1,0) (mm), the maximum temperature rise is reached at the end of the burst ($t = \tau$), although the value of T_{max} depends on the particular location. This is true for any point (0,y,0), with $|y| < l/2$. As we move past the crack tip, (for instance point (0,2,0) mm, another 1 mm further away from the center of the crack), the maximum temperature rise is drastically reduced and also delayed, occurring at $t_{max} > \tau$. These facts suggest that an analysis of the behaviour of T_{max} and t_{max} along the OY axis might be useful to determine the crack length. In the following subsections, we propose two methods, based on the analysis of $T_{max}(y)$ and $t_{max}(y)$, to estimate the length of the crack.

2.1 The t_{max} method

In Figure 3 we present the calculated t_{max} plot along the OY axis for two cracks of lengths l = 3 and 5 mm, in AISI-304, excited by a τ = 0.1 s burst.

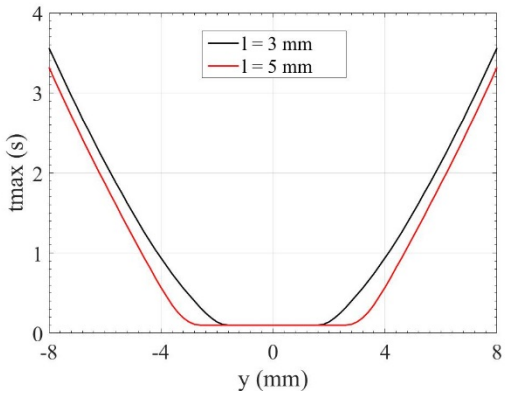

Figure 3. t_{max} profile along the direction of the crack (OY axis) of two cracks of lengths l = 3 (black) and 5 (red) mm in AISI 304, excited by a τ = 0.1 s burst.

A close inspection of Figure 3 reveals that, as soon as we move past the crack tip, the time at which the maximum temperature occurs, t_{max}, increases with respect to points belonging to the crack (for which $t_{max} = \tau$). This behaviour provides a method to measure the crack length that we will call "**the t_{max} method**", which consists in determining the position where t_{max} departs from the flat section characterized by $t_{max} = \tau$. The length covered by this flat section provides the length of the crack. However, when dealing with

experimental data, the determination of the length of the flat section is not straightforward due to the noise in the data. We will address this question in Section 3.

2.2 The T_{max} method

We focus now on the T_{max} dependence on coordinate y, i.e., along the surface line belonging to the crack plane. In Figure 4a we plot normalized theoretical T_{max} profiles along the OY direction for the same cracks as in Figure 3 (l = 3 and 5 mm, AISI-304), excited by the same burst (τ = 0.1 s).

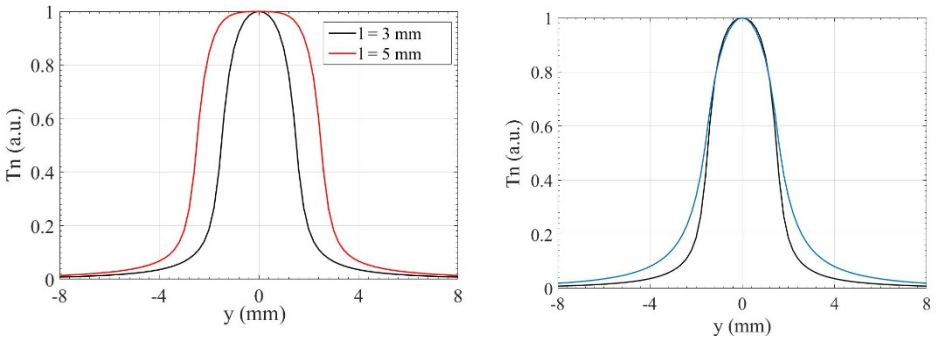

(a) (b)

Figure 4. (a) Normalized T_{max} profiles along the direction of the crack (OY axis) of two cracks of lengths l = 3 (black) and 5 (red) mm, excited by a τ = 0.1 s burst. (b) Normalized T_{max} profiles along the direction of the crack (OY axis) for a l = 3 mm long crack excited by two bursts of durations τ = 0.1 s (black) and τ = 0.5 s (blue)

If we compute the full width at half maximum (FWHM) of these curves, we find values of 3.0 and 5.0 mm, coinciding with the actual lengths of the cracks. These results point out that the FWHM of the T_{max} curve can be used to estimate the length of the crack We call this "**the T_{max} method**".

However, the duration of the burst has an impact on the T_{max} distribution along the OY axis. Figure 4b illustrates this dependence, for the l = 3 mm long crack, by considering two durations of the burst, namely, τ = 0.1 and 0.5 s. As can be seen, if we excite the crack with a τ = 0.5 s burst, the T_{max} curve is slightly wider than for a τ = 0.1 s burst excitation.

The value of FWHM of the curve corresponding to τ = 0.5 s is 3.4 mm, which overestimates the true length by about 13%. However, if we consider a longer crack, for instance l = 6 mm, the FWHM of the T_{max} curve corresponding to the same τ = 0.5 s burst

gives an excellent estimation of the crack width. These results indicate that there is a maximum burst duration that can be applied to estimate the length of a given crack, or that there is a minimum crack length that can be estimated with the T_{max} method for a given burst.

In order to quantify the dependence of FWHM of the T_{max} curve with the crack length l, in Figure 5a we compare FWHM values (obtained from $T_{max}(y)$ simulated curves for different lengths in AISI-304) and true lengths, for three bursts τ = 0.1, 0.2, and 0.5 s.

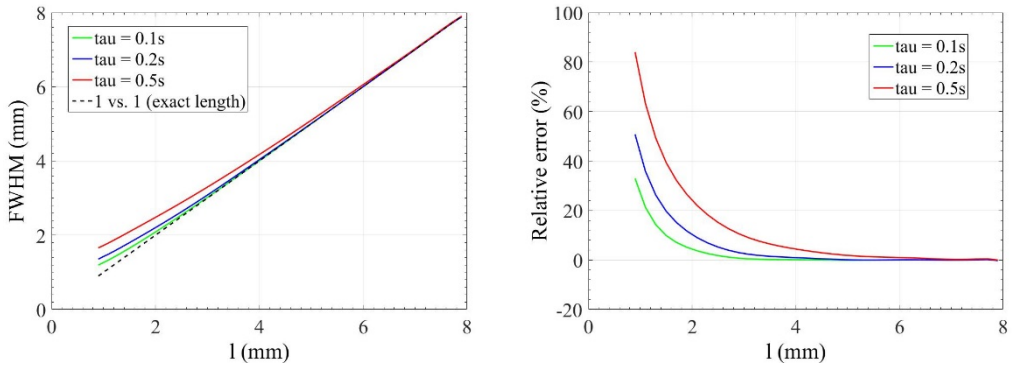

(a) (b)

Figure 5. (a) FWHM of the T_{max} curves as a function of the crack width, for bursts of duration τ = 0.1 s (green), 0.2 s (blue), and 0.5 s (red). The true crack widths are represented by the black dotted line. (b) Relative error in the estimation of the crack length from FWHM of the T_{max} curve, as a function of the crack length for the same bursts.

Figure 5a shows that, for long cracks, the relationship between the true crack length and the FWHM value is 1 to 1, so the FWHM value can be taken as a good estimation of the crack length. However, as the crack length is reduced, the FWHM value of the T_{max} curve overestimates the crack length, and the overestimation increases with the duration of the burst. In Figure 5b we display the relative error in the estimation of the crack length as a function of the true length, for the same bursts (τ = 0.1, 0.2, and 0.5 s). The curves show that the relative error increases dramatically when we reduce the length of the crack, especially for long bursts. As pointed out before, the results displayed in Figures 5a and 5b, indicate that, for a given burst duration τ, there is a minimum crack length that can be estimated accurately.

With the aim of determining the dependence of this minimum length on the burst duration τ, we have considered different definitions of “accurate length estimation”, namely, 1%, 2% and 5% error in the estimated length. Furthermore, in order to ensure the

universality of the conclusions in terms of materials' thermal properties, in Figure 6 we plot the minimum crack length as a function of the product $D\,\tau$.

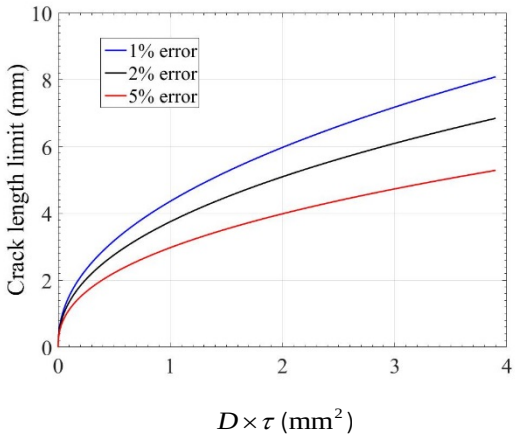

Figure 6. Minimum crack length that can be estimated with 1% (red) 2% (black) and 5% (blue) error from FWHM of the T_{max} curve as a function of the $D\,\tau$ product.

Figure 6 summarizes the conditions in which the length of a given crack in a particular material can be estimated with an error less than 1% (region above the blue line), 2% (region above the black line), and 5% (above the red line). For instance, in the case previously analyzed (AISI-304 and a burst duration of τ = 0.5 s) we can measure crack lengths down to l = 4 mm if we accept an error of 5%, but this minimum length increases up to l = 5.1 mm if we want the error to be less than 2% and to l = 6.1 mm if we want the error below 1%.

The results in Figure 6 also show that, in a given material, short cracks need shorter burst than long cracks in order for the length to be accurately estimated with the T_{max} method. Furthermore, the $D\tau$ degeneracy in Equation 1 indicates that a crack of a given length can be excited with a longer burst in a material with low conductivity than in a good thermal conductor.

We can conclude that we need to use short bursts to measure cracks with high precision using the T_{max} method. For example, bursts of τ = 0.1 s can be applied in AISI-304 to measure the length of cracks down to l = 2 mm long with a 5% accuracy. Although this conclusion might seem restrictive, we would like to recall that it has been shown that chaotic excitation in vibrothermography experiments provides a very efficient way of heating cracks and allows significant surface temperature elevation with bursts as short as τ = 0.05 s [32].

Finally, it is worth commenting on the effect of the crack penetration on the proposed methods. The calculations presented in this section correspond to cracks penetrating infinitely in the material. The results given by the t_{max} method are completely independent of the crack penetration, since the delay in reaching the maximum temperature past the crack tip occurs regardless of the penetration. In order to illustrate this, in Figure 7a we plot the t_{max} values along the *OY* axis for a l = 3 mm long crack in AISI 304 excited by a τ = 0.5 s burst and an infinite penetration, together with three finite penetrations of values h = 8, 4 and 2 mm.

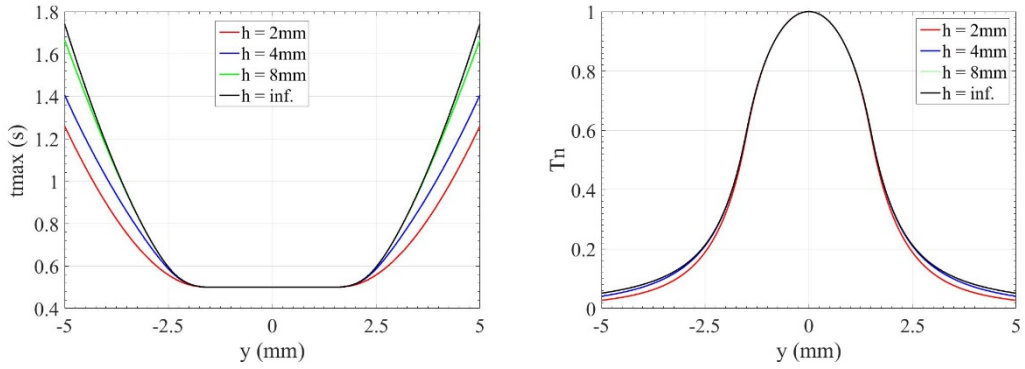

(a) (b)

Figure 7. Effect of the crack penetration on the (a) $t_{max}(y)$ and (b) $T_{max}(y)$ curves for l = 3 mm long cracks in AISI 304. An infinite penetrating crack (black line) is compared with cracks of penetrations h = 8 mm (green), h = 4 mm (blue) and h = 2 mm (red). The burst duration is τ = 0.5 s.

As can be observed, the signature of the t_{max} method, i.e., departure from the $t_{max} = \tau$ value beyond the crack tip is preserved in all cases, but the "wings" of the curve past the crack tip do depend on the penetration. An adequate calibration of these wings might be useful in future works to determine the penetration of the crack.

Regarding the T_{max} method, the differences in estimated crack lengths between deeply penetrating and shallow cracks are negligible for moderately long cracks. As an example, in Figure 7b we show T_{max} curves for the same length, burst and penetrations as in Figure 7a. As can be seen, for cracks down to h = 2 mm penetration, only far away from the crack the differences between the curves are barely noticeable, a region that is not significant for the crack length determination. The differences between FWHM values obtained for infinitely penetrating and shallow cracks are more significant for short cracks and long bursts. However, as the application of the T_{max} method requires short bursts, this is not a serious limitation. For instance, in the challenging case of a l = 1 mm long crack and a τ = 0.5 s burst, the FWHM values for an infinitely penetrating crack ($h = \infty$) and

finite penetrations of h = 2 mm and h = 1 mm differ by 5%, and 10%, respectively. Accordingly, we can say that l = 1 mm long cracks penetrating more than h = 2 mm behave as infinitely penetrating for τ = 0.5 bursts. However, if the crack is l = 3 mm long (as in Figure 7), it behaves as infinitely penetrating for h > 0.7 mm. Finally, cracks l = 5 and 7 mm long, as shallow as h = 0.2 mm, behave as infinitely penetrating for τ = 0.5 s bursts.

3. Experiments with calibrated samples

In order to test the validity of the T_{max} and t_{max} methods to determine crack lengths, we have performed burst vibrothermography experiments on samples containing artificial calibrated heat sources, representing fatigue cracks excited with ultrasounds.

3.1 Samples and equipment

In Figure 8 we show a diagram of the samples containing artificial heat sources that are excited in the experiment. They consist of two identical AISI-304 steel parts, each machined with a flat surface. We sandwich a thin (38 μm thick) Cu film of known length l (in the direction parallel to the sample surface) between the parts and attach them with screws. When we launch the ultrasounds, the friction between the Cu film and the steel flat surfaces produces heat, so a vertical heat source of known length l is excited in the experiment. In order to avoid any contact between the steel parts that would generate uncontrolled heat sources, we put two small Cu slabs at the back side of the plane containing the calibrated Cu film, so that they do not disturb the temperature we measure at the front surface. Under these conditions, the two flat steel surfaces are parallel, and we generate a homogeneous heat source of controlled dimensions corresponding to the area of the Cu film, perpendicular to the sample surface.

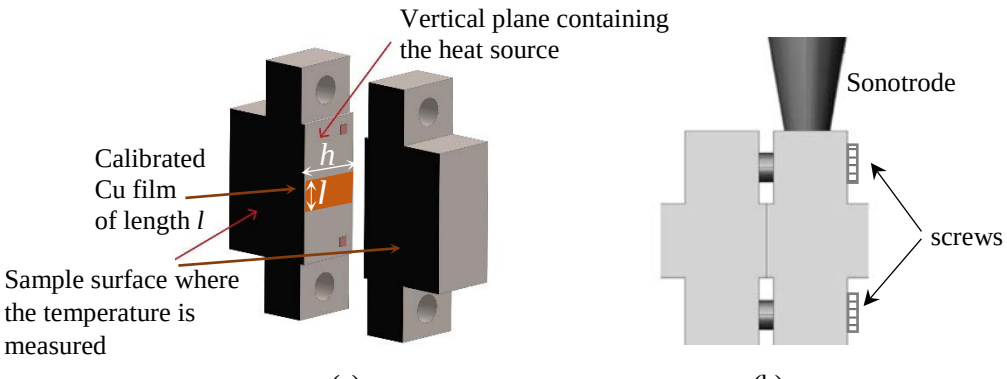

(a) (b)

Figure 8. (a) Diagram of the sample containing a calibrated heat source of length *l* excited in the experiment. (b) Diagram of the sample closed with screws, as viewed by the camera.

We have prepared Cu films with height h = 15 mm and different lengths l, ranging from 1 to 4 mm. We excite the sample with a tunable ultrasound system (15-25 kHz) with a maximum power of 20 kW (at 20 kHz). The sample is excited at an ultrasound frequency of 21.9 kHz , burst durations ranging from τ = 0.02 to 1 s and powers between 100 and 300 W. We cover the sample surface with a high emissivity paint and we insert a thin aluminium film between the sample and the sonotrode to improve ultrasound injection in the specimen.

The infrared radiation coming from the samples is captured by an infrared video camera (JADE, J550M from Cedip), working in the 3.5 to 5 μm range, at frame rates between 100 and 450 frames per second, depending on the duration of the burst. The camera is equipped with a 320 x 240 pixels detector and a 50 mm focal length lens. At the minimum working distance, the spatial resolution is 145 μm. In each film, the first frame is subtracted to obtain the temperature elevation above the ambient and to compensate for eventual emissivity inhomogeneities.

In order to illustrate the difficulty to size the length of a surface breaking crack from the direct visualization of single thermograms, we show in Fig. 9a the thermogram representing the temperature elevation above the ambient, generated by a Cu film of length l = 1.58 mm recorded at the end of a short burst of duration τ = 0.2 s. Figure 9b displays *OY* temperature profiles (white arrow in Figure 9a) before the injection of ultrasounds (t = - 0.01s) and at several instants of the sequence, during and after the excitation, namely, t = 0.02, 0.05, 0.1, 0.2 s and 0.4 s. As can be observed, heat diffusion produces a temperature distribution from which the crack length is impossible to be determined. More precisely, the profiles depicted in Figure 9b illustrate the continuous evolution of this temperature distribution and therefore the inability to pick one single thermogram to evaluate the length of the crack. The methodology we are proposing in this work is addressed to overcome this issue by making use of the whole image sequence to determine the crack length accurately.

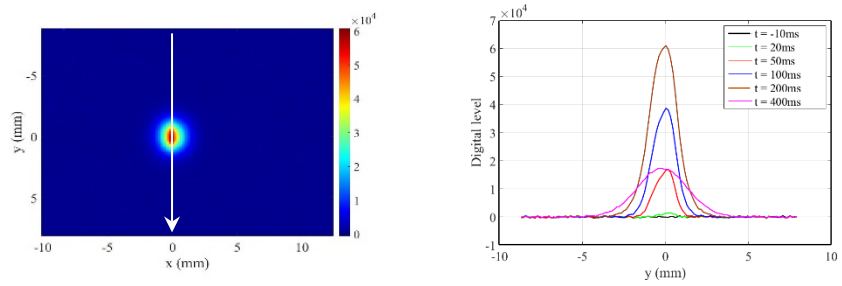

(a) (b)

Figure 9. (a) Experimental thermogram generated with an l = 1.58 mm long Cu film, excited with a τ = 0.2 s burst, obtained at $t = \tau$ = 0.2 s. (b) *OY* temperature profiles (white arrow in Figure 9a) corresponding to thermograms recorded at t = -0.01, 0.02, 0.05, 0.1, 0.2, and 0.4 s in the same sequence.

3.2 Results of the t_{max} method

In Figure 10a we illustrate the results of the t_{max} method by showing a t_{max} surface map corresponding to data obtained with an l = 2.2 mm long Cu film excited with a τ = 0.2 s burst. In Figure 10b we present t_{max} profiles along the *OY* axis (white arrow in Figure 10a), for the same slab excited with bursts of durations τ = 0.08, 0.1, 0.2, 0.4, and 0.8 s.

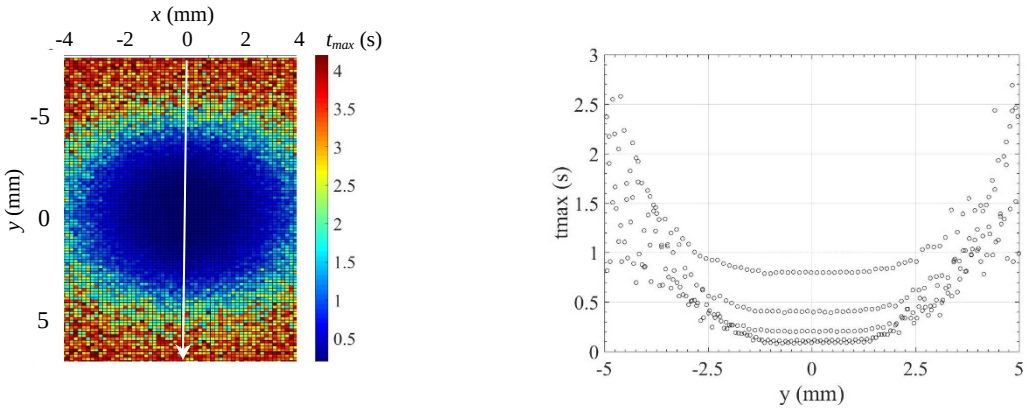

(a) (b)

Figure 10. (a) Experimental t_{max} surface map for an l = 2.2 mm long Cu film, excited with a τ = 0.2 s burst. (b) Experimental t_{max} profiles along the *OY* axis for the same Cu film, excited with bursts of duration τ = 0.08, 0.1, 0.2, 0.4, and 0.8 s (from bottom to top).

As predicted by the theory, t_{max} *OY* profiles exhibit a flat section with values around $t_{max} = \tau$ along the crack length, and beyond the crack tip, t_{max} values increase. However, as pointed out in section 2.1, experimental $t_{max}(y)$ curves are affected by noise, which makes it challenging to determine the position of the crack tip, and consequently, to estimate the crack length.

In order to implement the t_{max} method on experimental data, we have established the following methodology. (a) Select the central points of the crack, located well within the flat region. (b) Compute the mean t_{max}, $< t_{max} >$, and the standard deviation, σ, of these points. (c) Determine that the points belonging to the crack are those with a t_{max} value smaller than $< t_{max} > + \sigma$.

This methodology has been settled after studying several alternatives regarding the criterion to determine which points belong to the crack. We have considered three possibilities: the points belonging to the crack are the ones that have a t_{max} smaller than (1) $< t_{max} > + 0.5\ \sigma$, (2) $< t_{max} > + \sigma$, and (3) $< t_{max} > + 2\sigma$. As an example, Figure 11 illustrates the application of the three criteria to the estimation of the length of the l = 2.2 mm Cu film.

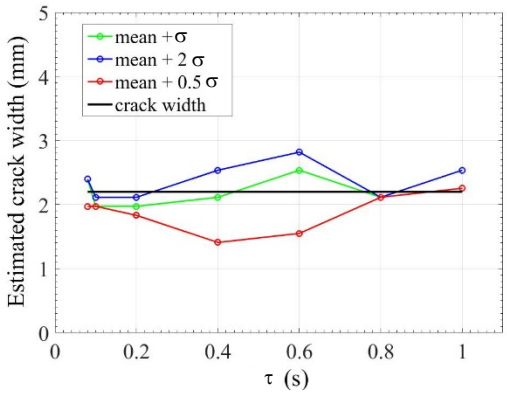

Figure 11. Estimated crack length by considering $< t_{max} > + 0.5\ \sigma$ (red), (2) $< t_{max} > + \sigma$ (green), and (3) $< t_{max} > + 2\sigma$ (blue), for a Cu film of actual length (horizontal black) l = 2.2 mm.

As can be observed, the criterion based on $< t_{max} > + 0.5\ \sigma$, underestimates the crack length whereas the $< t_{max} > + 2\sigma$, criterion overestimates it. The criterion based on $< t_{max} > + \sigma$ provides the best estimation of the length of the crack, so it has been adopted as the optimum choice.

We also took data on samples containing Cu films of other lengths, namely l = 1.58 and 3.55 mm, that we excited with different bursts ranging from τ = 0.1 to 1 s. The resulting crack lengths estimated by the t_{max} method are summarized in Tables 1, 2 and 3.

The results on the second columns of Tables 1, 2, and 3 show that the t_{max} method is quite robust in terms of providing adequate results independently of the duration of the burst. However, when the noise level is high, the crack length is underestimated because, close to the crack tip, the reduction of the signal level makes the determination of the time for maximum temperature more uncertain, and thus it is more likely to find points that

exceed $< t_{max} > + \sigma$. This is why short bursts, which produce a reduced temperature elevation, are more likely to give underestimated results, although, this underestimation can also take place for longer bursts if the quality of the data is poor. Anyway, the results prove that the criterion based on $< t_{max} > + \sigma$ provides a very adequate estimation of the crack length from the t_{max} method.

3.3 Results of T_{max} method

We have also tested the T_{max} method with experimental data. As an example, in Figure 12a we present the T_{max} surface map obtained by exciting a Cu film l = 1.58 mm long with a τ = 0.2 s. The corresponding normalized T_{max} profile along the *OY* axis (white arrow in Figure 12a), together with the simulated profile for the same crack length and burst duration, are depicted in Figure 12b.

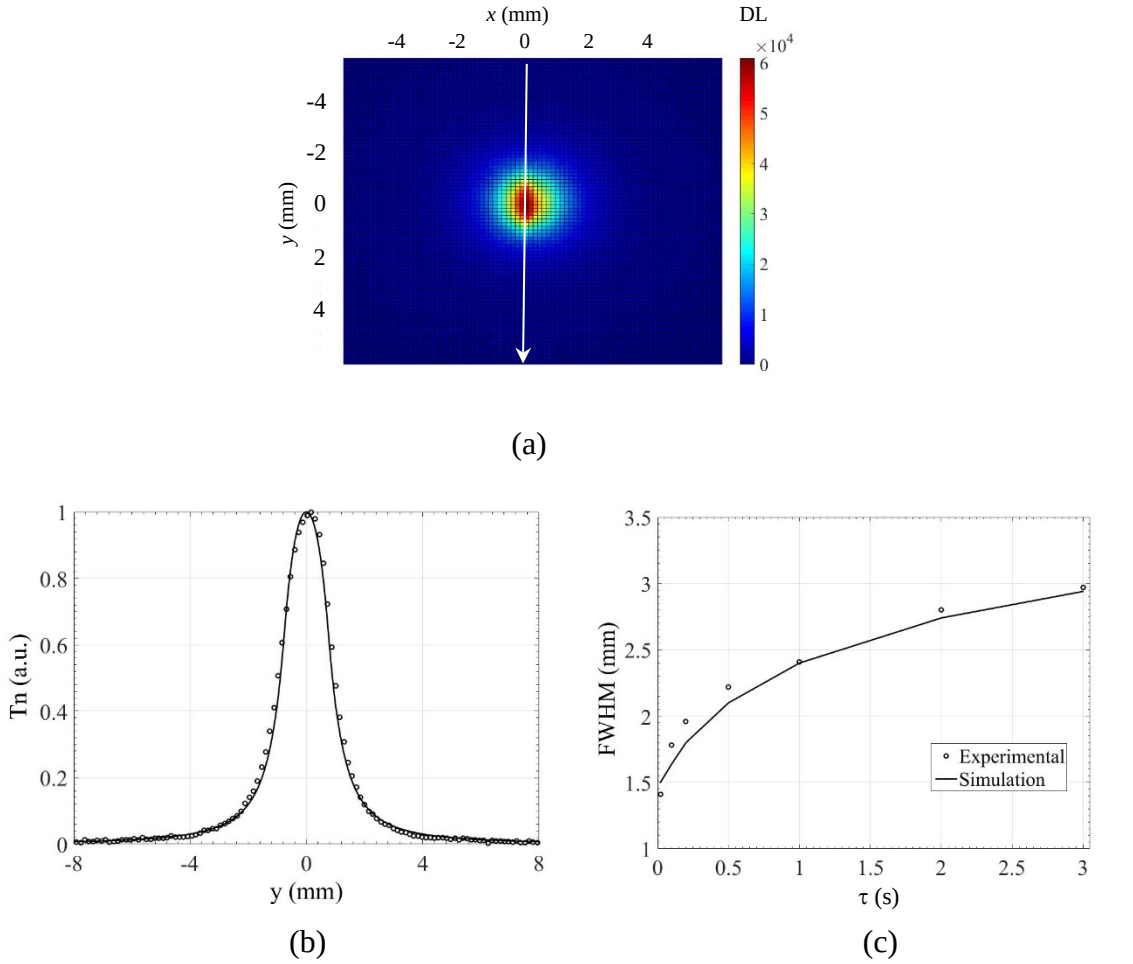

Figure 12. (a) Experimental T_{max} surface map obtained with an l = 1.58 mm long Cu film excited with a τ = 0.2 s burst. (b) Experimental (symbols) and theoretical (solid line) T_{max} profile along the *OY* direction (white arrow in (a)). (c) Experimental (symbols) and theoretical (solid line) FWHM values of the T_{max} profile along the *OY* direction for the same Cu film excited with different bursts.

As can be seen, the coincidence between the experimental data and the theoretical prediction is very accurate.

The same artificial crack was excited with different bursts. In Figure 12c we plot the values of FWHM of $T_{max}(y)$ profiles obtained for different bursts, together with the values predicted by the theory. For all burst durations τ explored, the coincidence is again very good, with a slight overestimation in experiments.

We also applied the T_{max} method to the data collected on samples containing Cu films of other lengths (l = 2.2 and 3.55 mm), excited with bursts ranging from τ = 0.1 to 1 s. The estimated crack lengths from FWHM results for the three cracks analysed are summarized on the last columns of Tables 1, 2 and 3. As can be seen, the method provides good estimations of the crack length for short bursts. As predicted in Figure 6, the maximum burst for which we obtain an accurate length estimation with the T_{max} method increases with the crack length. Note that, in order to test the capability of the method, we have performed experiments on short cracks, which are the most challenging to size. It is worth recalling that the spatial resolution in these experiments is 145 μm, which represents a 9% of the shortest crack length l = 1.58 mm, and about 7% of the l = 2.2 mm long crack. Thus, the deviations of the estimated crack lengths from the real values are not only affected by the methodology itself, but also by the spatial resolution. The results could be improved using a high resolution camera or a microscope lens. Accordingly, we can say that the experimental results follow the theoretical predictions in Figure 6. It is worth mentioning that the processing of the data takes about 25 seconds in a laptop.

Table 1. Results for l = 1.58 mm. τ is the burst time, and l_{tmax} and l_{Tmax} and are the lengths computed with the t_{max} and T_{max} methods, respectively. Color code: green for error <10% with respect the actual length; orange for error 10-20% and red for error >20%. Resolution of 0.145 mm

τ (s)	l_{tmax} (mm)	l_{Tmax} (mm)
0.02	1.1	1.5
0.1	1.5	1.7
0.2	1.5	2
0.5	1.5	-
1.0	1.6	-

Table 2. Results for l = 2.2 mm. Same symbols, color code and resolution as in Table 1.

τ (s)	l_{tmax} (mm)	l_{Tmax} (mm)
0.08	-	2.3
0.1	2.0	2.4
0.2	2.0	2.6
0.4	2.1	2.9
0.8	2.1	-

Table 3. Results for l = 3.55 mm. Same symbols, color code and resolution as in Table 1.

τ (s)	l_{tmax} (mm)	l_{Tmax} (mm)
0.1	-	3.7
0.2	3.2	3.8
0.3	3.2	3.9
0.5	3.3	4.1
0.7	3.5	4.3
0.8	3.3	-
0.9	3.5	-
1.0	3.8	-

As a summary, the results displayed in Tables 1, 2 and 3 indicate that the t_{max} method is quite robust in terms of providing adequate results independently of the duration of the burst. However, when the noise level is high the crack length is underestimated because close to the end of the crack, the reduction of the signal level makes the determination of the time for maximum temperature more uncertain and thus it is more likely to find points that exceed $< t_{max} > + \sigma$. This is why short bursts, which produce a reduced temperature elevation, are more likely to give underestimated results.

The T_{max} method is more predictable as it consistently provides good results for short enough bursts, regardless of the quality of the data. This makes this method fully trustable with short bursts. It should be noted that the typical deviations appearing in both methods occur in opposite directions: whereas the t_{max} method underestimates the length of the crack with poor quality data, the T_{max} method systematically overestimates it if the burst is not short enough. This suggests that a cross-check of the results produced by both methods is the guarantee of an accurate estimation of the crack length. Furthermore, for an optimum evaluation of the crack length, the comparison should be done between the results given by experiments designed according to the optimal performance of each method: a good signal to noise ratio (usually implying a long burst) for the t_{max} method

and the shortest possible burst for the T_{max} method. Thus, in the challenging cases of short cracks, performing two experiments at two different bursts, one short (below τ = 0.1 s) and one long (above τ = 1 s) burst, might be necessary for an accurate estimation of the crack length. According to the results displayed in tables 1, 2, and 3, a discrepancy of less than 10 % between both methods ensures an accurate estimation of the crack length.

4. Summary and conclusions

UET can be efficiently applied to evaluate the length of fatigue-like cracks by analyzing the temperature evolution at the surface along a line profile containing the crack. The proposed methods consist in analyzing two quantities along this profile: the maximum temperature reached at each position and the time at which the maximum temperature occurs. It has been shown that the time at which the maximum temperature occurs coincides with the duration of the burst at points of the surface which belong to the crack but beyond the crack tip the maximum temperature is reached later. Furthermore, the FWHM of the maximum temperature curve provides the crack length for short enough bursts or long enough cracks. The crack length and burst durations for which the method is valid have been analyzed theoretically, providing universal curves that establish the longest bursts that can be applied to size a certain crack in a given material. The methodology has been applied to samples containing artificial calibrated cracks. The results indicate that the quality of the data is crucial for the t_{max} method to provide accurate length values. As short bursts give rise to poorer quality data, the crack widths are likely to be underestimated. It is worth stressing that this is not a limitation of the t_{max} method itself, but to the quality of the data that short bursts produce. On the opposite, the T_{max} method provides better results with short bursts. The combination of both methods ensures the reliability of the results when they provide similar estimations of the crack length within a 10% uncertainty. In experimental situations where either long or short bursts are preferred, just applying the t_{max} or the T_{max} method, respectively, ensures an accurate estimation of the crack length. As a conclusion, we can say that it is possible to size the length of surface breaking vertical cracks using UET without the need of performing complicated inversion procedures. The methodology will be next applied to measure the length of real fatigue cracks.

Acknowledgments

This work has been supported by Ministerio de Economía y Competitividad (DPI2016-77719-R, AEI/FEDER, UE), by Gobierno Vasco (PIBA2018/15) and by Universidad del País Vasco UPV/EHU (GIU16/33).

REFERENCES

[1] R. Jones, “Fatigue crack growth and damage tolerance”, Fatigue Fract. Eng. Mat. Struct. 37, 463-483 (2014).

[2] F. Ancona, D. Palumbo, R. De Finis, G. P. Demelio, U. Galietti, “Automatic procedure for evaluating the Paris Law of martensitic and austenitic steels by means of thermal methods”, Engineering Fracture Mechanics, 163, 206-219 (2016).

[3] D. Palumbo, R. De Finis, F. Ancona, U. Galietti, “Damage monitoring in fracture mechanics by evaluation of the heat dissipated in the cyclic plastic zone ahead of the crack tip with thermal measurements”, Engineering Fracture Mechanics, 181, 65-75 (2017).

[4] R. A. Tomlinson, E. J. Olden, “Thermoelasticity for the analysis of crack tip stress fields – a review” Strain, 35, 49-7 (1999).

[5] F. A. Diaz, E. A. Patterson, R. A. Yates, “Some improvements in the analysis of fatigue cracks using thermoelasticity” Int. J. Fatigue 26(4) 365–12 (2004).

[6] J. Schlichting, Ch. Maierhofer, M. Kreutzbruck, “Crack sizing by laser excited thermography” NDT&E Int. 45, 133–140 (2012).

[7] M. Streza, Y. Fedala, J. P. Roger, G. Tessier, C. Boue, “Heat transfer modeling for surface crack depth evaluation”, Meas. Sci. Technol. 24, 045602 (2013).

[8] N. W. Pech-May, A. Oleaga, A. Mendioroz, A. J. Omella, R. Celorrio, A Salazar, “Vertical cracks characterization using lock-in thermography: I infinite cracks”, Meas. Sci. Technol. 25, 115601 (10pp) (2014).

[9] N. W. Pech-May, A. Oleaga, A. Mendioroz, A. Salazar, “Fast Characterization of the width of vertical cracks using pulsed laser spot infrared thermography”, J. Nondestr. Eval. 35, 22 (2016).

[10] T. Li, D. P. Almond, D. A. S. Rees, “Crack imaging by scanning laser-line thermography and laser-spot thermography”, Meas. Sci. Technol. 22, 035701 (2011).

[11] T. Li, D. P. Almond, D. A. S. Rees, “Crack imaging by scanning pulsed laser spot thermography” NDT&E Int. 44, 216–225 (2011).

[12] J. Rantala, D. Wu, G. Busse, “Amplitude-modulated lock-in vibrothermography for NDE of polymers and composites” Res. Nondestr. Eval. 7, 215-228 (1995).

[13] A. Mia, X. Han, S. Islam, G. Newaz, “Fatigue damage detection in graphite/epoxy composites using sonic infrared imaging technique” Comp. Sci. Tech. 64 657-666 (2004).

[14] T. J. Barden, D. P. Almod, S. G. Pickering, M. Morbidini, P. Cawley, “Detection of impact damage in CFRP composites by thermosonics” Nondestr. Test. Eval. 22 71-82 (2007).

[15] H. Fernandes, C. Ibarra-Castanedo, H. Zhang, X. Maldague, “Thermographic nondestructive evaluation of carbon fiber reinforced polymer plates after tensile testing” J. Nondestr. Eval. 34:35 1-10 (2015).

[16] M. Morbidini, P. Cawley, T. Barden, D. Almond, P. Duffour, “Prediction of the thermosonic signal from fatigue cracks in metals using vibration damping measurements” J. Appl. Phys. 100 104905 (13pp) (2006).

[17] S. D. Holland, C. Uhl, Z. Ouyang, T. Bantel, M. Li, W. Q, Meeker, J. Lively, L. Brasche, D. Eisenmann, “Quantifying the vibrothermographic effect” NDT&E Int. 44 775-782 (2011).

[1] R. Montanini, F. Freni, G. L. Rossi, “Quantitative evaluation of hidden defects in cast iron components using ultrasound activated lock-in vibrothermography” Rev. Sci. Instr. 83 094902 (8pp) (2012).

[19] L. D. Favro, X. Han, Z. Ouyang, G. Sun, R. L. Thomas, “Sonic IR imaging of cracks and delaminations” Analitical Sciences 17 451-453 (2001).

[20] R. Montanini, F. Freni, G. L. Rossi,” Quantitative evaluation of hidden defects in cast iron components using ultrasound activated lock-in vibrothermography” Rev. Sci. Instr. 83 094902 (8pp) (2012).

[21] X. Guo, V. Vavilov, Crack detection in aluminum parts by using ultrasound excited infrared thermography Infr. Phys. Tech. 61 149-156 (2013).

[22] A. Mendioroz, R. Celorrio, A. Salazar, “Ultrasound excited thermography: an efficient tool for the characterization of vertical cracks”, Rev. Sci. Instr. 28, 112001 (27 pp) (2017).

[23] R. Celorrio, A. Mendioroz, A. Salazar, “Characterization of vertical buried defects using lock-in vibrothermography: II. Inverse problem” meas. Sci. Technol. 24, 6, 065602 (2013).

[24] A. Mendioroz, A. Castelo, R. Celorrio, A. Salazar, “Characterization and spatial resolution of cracks using lock-in vibrothermography”, NDT&E Int. 66, 8-15 (2014).

[25] A. Castelo, A. Mendioroz, R. Celorrio, A. Salazar, “Optimizing the Inversion Protocol to Determine the Geometry of Vertical Cracks from Lock-in Vibrothermography”, J. Nondestr. Eval. 36, 1 (2017).

[26] A. Castelo, A. Mendioroz, R. Celorrio, A. Salazar, P. López de Uralde, I. Gorosmendi, E. Gorostegui-Colinas “Characterizing open and non-uniform vertical heat sources: towards the identification of real vertical cracks in vibrothermography experiments” THERMOSENSE: THERMAL INFRARED APPLICATIONS XXXIX, Proceedings of the SPIE 10214, 1021401 (2017).

[27] R. Celorrio, A. Mendioroz, A. Cifuentes, L. Zaton, A. Salazar, “Sizing vertical cracks using burst vibrothermography”, NDT&E Int. 84, 36-46 (2016) .

[28] A. Mendioroz, K. Martínez, R. Celorrio, A. Salazar, “Characterizing the shape and heat production of open vertical cracks in burst vibrothermography experiments” NDT&E International 102, 234-243 (2019).

[29] Z. Ouyang, L. D. Favro, R. L. Thomas, X. Han, “Theoretical modeling of thermosonic imaging of cracks” AIP Conf. Proc. 21, 577-581 (2002).

[30] B. A. Abu-Nabaha, S. M. Al-Saidb, R. Gouia-Zarrad, “A simple heat diffusion model to avoid singularity in estimating a crack length using sonic infrared inspection technology”, Sensors &Actuators A: Physical, 293, 77–86 (2019).

[31] A. Mendioroz, R. Celorrio, A. Salazar, “Characterization of rectangular vertical cracks using burst vibrothermography”, Review of Scientific Instruments 86, 064903 (2015).

[32] X. Han, Z. Zeng, W. Li, S. Islam, J. Lu, V. Loggins, E. Yitamben, L. DL. Favro, G. Newaz, R. L. Thomas, “Acoustic chaos for enhanced detectability of cracks by sonic infrared imaging” J. Appl. Phys. 95 (7), 3792-3797 (2004).